Arch. Metall. Mater. **66** (2021), 2, 407-418

DOI: 10.24425/amm.2021.135872

S. AMARES[1,2*], R. DURAIRAJ[2], S.H. KUAN[2]

EXPERIMENTAL STUDY ON THE MELTING TEMPERATURE, MICROSTRUCTURAL AND IMPROVED MECHANICAL PROPERTIES OF SN58BI/CU SOLDER ALLOY REINFORCED WITH 1%, 2% AND 3% ZIRCONIA (ZrO_2) NANOPARTICLES

This paper investigates the influence of 1%, 2% and 3% zirconia (ZrO_2) nanoparticles to the melting, microstructural and mechanical properties of the Sn58Bi solder. Melting temperatures of 145.11°C, 140.89°C and 143.84°C were attained correspondingly for the 1%, 2% and 3% ZrO_2 reinforced Sn58Bi solder. The microstructures especially the spacing between the lamellar structures of the Sn58Bi solder alloy was narrower for 1% ZrO_2 added with Sn58Bi solder alloy. The highest and lowest hardness value of 32.28 HV and 27.62 HV was recorded for 1% and 2% ZrO_2 additions respectively. Highest shear strength value was noted for the 3% ZrO_2 added SnBi/Copper joint with 0.8712 kN, while the lowest value of 0.4380 kN noted for the 1% ZrO_2 added SnBi/Copper joint. The presence of small-sized ZrO_2 nanoparticles can be seen to be properly dispersed at the solder joint to increase the shear load at maximum joint stress.

Keywords: SnBi solder, low melting temperature, microstructure, hardness, shear load

1. Introduction

In current soldering technology era, the alloying process contributes to the enhancement of solder alloy, where the metal elements are added to the base metal of tin (Sn). Commonly, the alloying process increases the performance of solder alloy through melting temperature (e.g. tin-plumbum, tin-bismuth), shear strength (e.g. tin-zinc-bismuth) and enabling long-term reliability (e.g. tin-argentum-copper) due to better joint property. However, to date, several research groups were focused on the addition of micro and nanoparticles, for example metallic e.g., argentum (Ag) [1], indium (In) [2], nickel (Ni) [3], aluminium (Al) [4], cobalt (Co) [5] etc. and ceramic e.g., titanium dioxide (TiO_2), aluminium oxide (Al_2O_3), zirconia (ZrO_2) and cerium oxide (Ce_2O_3) and etc. [6-9] particles into Sn-based solder alloys. The nanoparticles are known to be in mini size, less in weight and density that enable the electronic device to be produced in a miniaturized design that accommodates to the latest trend of smaller electronic devices. Therefore, solder alloys with the additions of nanoparticles are vastly investigated in terms of the melting temperature (low melting temperature), microstructure (grains sizes, intermetallic compound (IMC) production, eutectic area), mechanical (hardness, shear/tensile strength), wettability (spreading on substrate) and interfacial (thin IMC layer) properties [10,11].

Currently, many researches opted in studying the effect of various nanoparticles reinforcement in the SnAgCu (SAC) solder alloy. Increase in the tensile strength and suppression of IMC layer was revealed with additions of TiO_2 into Sn0.7Cu [12]. Separately, [13] established an increase in the hardness value to the Sn3.0Ag0.5Cu with presences of iron nickel oxide (Fe_2NiO_4), iron oxide (Fe_2O_3), nickel oxide (NiO), and indium tin oxide (ITO) and carbon nanostructure diamond (C). Similar effect was reported by [14] with additions of NiO particles (0.5, 1.5, and 2.5% by weight) in the Sn3.0Ag0.5Cu solder. In another study carried out by [15], microstructural properties were improved with the production of smaller Ag_3Sn grains in the Sn3.5Ag0.5Cu solder upon addition of 0.7 wt.% zinc oxide (ZnO) nanoparticles. The IMC growth was hindered by 0.1 wt.% TiO_2 in the Sn3.0Ag0.5Cu solder as the nanoparticles accumulated in the interfacial layer as clarified by [15]. [7] added 1 wt.% ZrO_2 nanoparticles into the Sn9Zn which was soldered to the Ni/Au BGA pad. The ZrO_2 nanoparticles suppressed the NiSn IMC particle's growth at the solder joint to increase the shear load

[1] UNIVERSITI TUNKU ABDUL RAHMAN, LEE KONG CHIAN FACULTY OF ENGINEERING AND SCIENCE, JALAN SUNGAI LONG, BANDAR SUNGAI LONG, 43000 KAJANG, SELANGOR, MALAYSIA
[2] CENTER OF MECHANICAL AND MATERIALS ENGINEERING, FACULTY OF ENGINEERING AND BUILT ENVIRONMENT, SEGI UNIVERSITY NO. 9, JALAN TEKNOLOGI, TAMAN SAINS SELANGOR, KOTA DAMANSARA PJU 5, 47810 PETALING JAYA, SELANGOR, MALAYSIA

* Corresponding author: amaressinghgill@segi.edu.my

from 1108 g to 1126 g, even with a slightly thicker IMC layer observed in comparison to the bare solder. This statement was also reported by [16] with additions 0.5 wt% and 1.0 wt% ZrO_2 nanoparticles to the Sn3.0Ag0.5Cu. The research stressed out that the presences of ZrO_2 did not significantly change the IMC layer, but the higher content of the ZrO_2 nanoparticles contributes to higher shear strength. Following that, being a ceramic material, the ZrO_2 is unreacted to the Sn, Ag and Cu which helped in the reduction of Cu_3Sn-Cu_6Sn_5 IMC layer thickness. However, many studies also emphasise that higher amount of nanoparticles tends to reduce the efficient trend by deteriorating the strength [17-19]. It was stated that the addition of nanoparticles acts as separate/discrete particles for ceramics nanoparticles [20,21].

Recent studies have shown that the incorporation of ceramics nanoparticles into solder alloys enhances the properties but not many have speculated about the effect of adding ceramics and metal nanoparticles into low-melting solder alloys. Nevertheless, few studies have been conducted on the low melting solder system such as the SnBi solder system. In one study, graphene nanosheets (GNS) were used as the reinforced particles to the Sn58Bi solder. The increase of hardness was evident with a jump from 309 MPa to 380 MPa for the GNS added solder [22]. There was no major change in the melting temperature for the Sn58Bi upon adding the GNS particles but refinement of the microstructure was evident. Adding Ag nanoparticles into the Sn58Bi solder alloy recorded shear strength 21% higher than the bare Sn58Bi solder as reported by [23]. Refining strengthening and dispersion strengthening with the Ag_3Sn IMC nanoparticles influences the hike in the shear strength. The molybdenum (Mo) nanoparticles was incorporated into the Sn58Bi solder alloy and the tensile strength was improved [24]. The Mo nanoparticles appear to be bypassed by the dislocation due to the characteristics of the hard Mo particles that could not be penetrated causing the dislocation to pile up and improving the mechanical strength. The pinning effect of the Zn nanoparticles in the Sn58Bi increase the tensile strength [25].

The mixed research of nanoparticles additions into the low temperature SnBi solder alloy is somewhat general with limited research using ceramics nanoparticles additions. Thus, this research examines the melting temperature, microstructure, mechanical (hardness and shear strength) of a low-temperature solder alloy, Sn58Bi (SB) added with 1%, 2% and 3% ZrO_2 nanoparticles. The results obtained from the attribution of ZrO_2 nanoparticles in SB promote the novelty of this study. Studying the effect of the ceramic ZrO_2 nanoparticles additions to the low temperature solder alloy closes the research gap with other numerous studies done to higher melting point solder alloy such as SnAgCu.

2. Experimental procedure

The material for this Sn58Bi (SB) solder alloy preparation was prepared from tin (Sn) (99.9% pure – Sigma Aldrich), bismuth (Bi) (99.9% pure – Sigma Aldrich) and zirconia (ZrO_2) nanoparticles (99.9% – Sigma Aldrich). Three samples each with 11.6 g Bi and 8.48 g Sn were put together in three different crucibles. These crucibles were added with ZrO_2 nanoparticles of 1, 2 and 3% weight percentage each from the total of 20 g of Sn and Bi. All solders were inserted together in alumina crucible separately according to the weight percentage. These samples were put in an induction vacuum furnace (Carbolite Furnace RHF 15/8) with the temperature profile as depicted in Fig. 1(a). The molten solder alloys with ZrO_2 nanoparticles were let to solidify at room temperature to imitate the cooling effect experienced by the solders in the industry. Prior to the addition of the nanoparticles, the ZrO_2 particle size was calculated with an average of 29.7 nm as shown in Fig. 2. The SB solder alloy added with 1%, 2% and 3% ZrO_2 were subsequently re-melted at 350°C using a hotplate for 20 minutes with mechanical stirring to ensure a homogenous mixture of the nanoparticles. During this process, aluminium foils were designed to cover the alu-

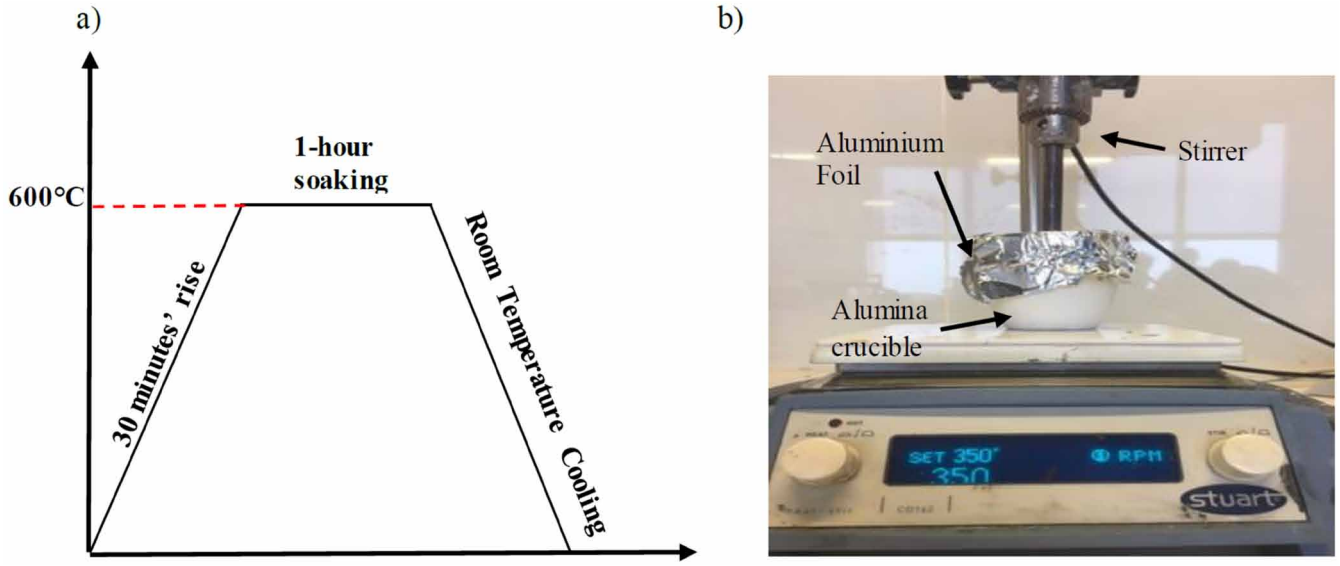

Fig. 1. a) Temperature profile and b) Stirring setup

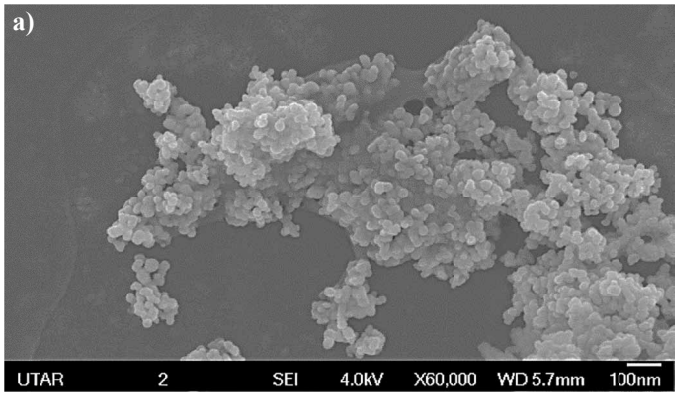

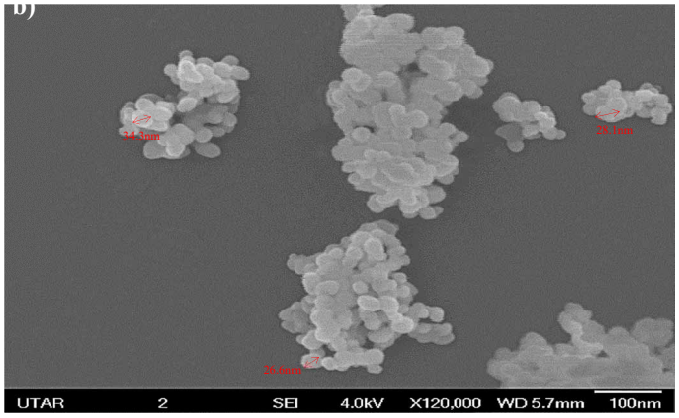

Fig. 2. FESEM images of ZrO_2 nanoparticles size after immersed in ethanol at a) × 60000 and b) × 120000 magnifications

mina crucible to avoid oxidation as shown in Fig. 1(b). These nanocomposite solders are denoted by SB + 1, 2 and 3% of ZrO_2 onwards in this paper. The solder alloys were cut into billets with dimensions of 50 mm × 10 mm after remelting. Such small dimension will replicate the less mass consumed solder paste in the electronic industry and at the same time reduce the wastage of raw materials. Samples of 5 mg for each SB + 1, 2 and 3% of ZrO_2 were used for the melting temperature analysis using differentials scanning calorimetry machine (DSC 4000-Perkin Elmer). The heat flow for all solder alloys was kept at 20°C/min with temperature range from 100°C to 600°C under Nitrogen (N) atmosphere. The Vickers hardness test using the Wolpert Wilson Vickers 432-SVD tester was conducted by taking five measurement indentations from each percentage of addition of solder alloy with 1 kgf indentation load. The shear strength of the SB + 1, 2 and 3% of ZrO_2 was determined in accordance with the ASTM D1002 (single shear lap joint). The SB + 1, 2 and 3% of ZrO_2 were soldered onto the copper (Cu) substrate with dimensions of 40 mm × 5 mm × 10 mm which is as shown in Fig. 3. The soldering temperature was maintained at 230°C for 60 seconds. The zinc chloride (ZnCl) flux was used to reduce oxidation to disregard any external influences on the properties. The crosshead speed was decided as the fixed variable with 1.3 mm/min in accordance with the ASTM D1002 to ensure that no other parameter influences the shear strength except the solder and ZrO_2 nanoparticles. The Universal Testing Machine (Instron 5582Q4970) was utilized for the shear test. Usually, the strain

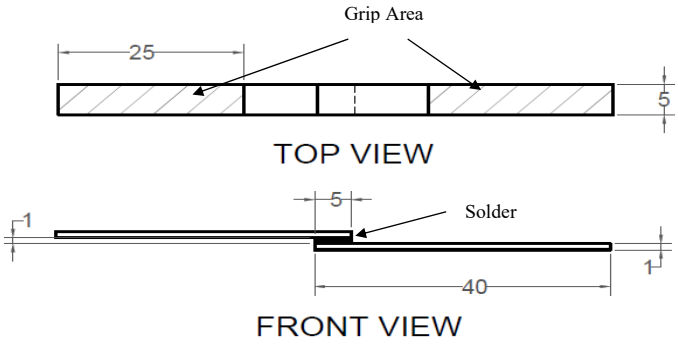

Fig. 3. Single lap shear specimen

rate effects the shear strength of a solder joint but as clarified, this research examines only the effect of adding ZrO_2 with the solder on the solder joint.

3. Results and discussions

3.1. Melting temperature

Investigation on the thermal properties of the SB and SB + 1, 2 and 3% ZrO_2 showed the melting peaks as depicted in Figs. 4 while the values are listed in Table 1. All graphs showed sharp endothermic peak resulted from the energy used for breaking of the bonds. The additions of nanoparticles to the solder provided a mixed trend in terms of melting temperature. The solder with 2% ZrO_2 addition produced lower melting point of 140.89°C compared to the other two percentages of addition and bare SB solder alloy. However, the solder remained in the molten liquid form and slightly longer as it only completely melted at 145.15°C, producing a greater pasty range. An additional peak was observed in Fig. 2(b) for the 2% ZrO_2 additions indicating the attendance of ZrO_2 nanoparticles that disrupts the melting of the SB solder. Such appearance happens as a result of some part of the SB solder melting earlier and with some other part of the solder still existing as solid. Appearance of this peaks was also observed in the study by [25] for the SnAgZn solder system and according to the research, the peak resembles the existence of both liquid and solid phase during the melting process. This phenomenon also proves the occurrence of local dissolution of the ZrO_2 nanoparticles in the molten SB solder in conjunction to the study by [6], whom likewise found two peaks in the DSC curve with additions of TiO_2 nanoparticles in the Sn3.50.25AgCu solder. The highest melting point of 145.11°C was obtained by the 1% ZrO_2 added into SB solder alloy which completely melted at 148.82°C, faster than the SB solder. The 3% ZrO_2 added into SB solder alloy started to melt at 143.84°C and completely melted at 147.44°C. The trend of the solidus and liquidus temperature is shown in Fig. 5. In analysing the melting properties of any solder alloy, the melting point and pasty range are the major concern.

Melting points of any newly developed solder alloys are compared usually with the traditional lead solder as this solder

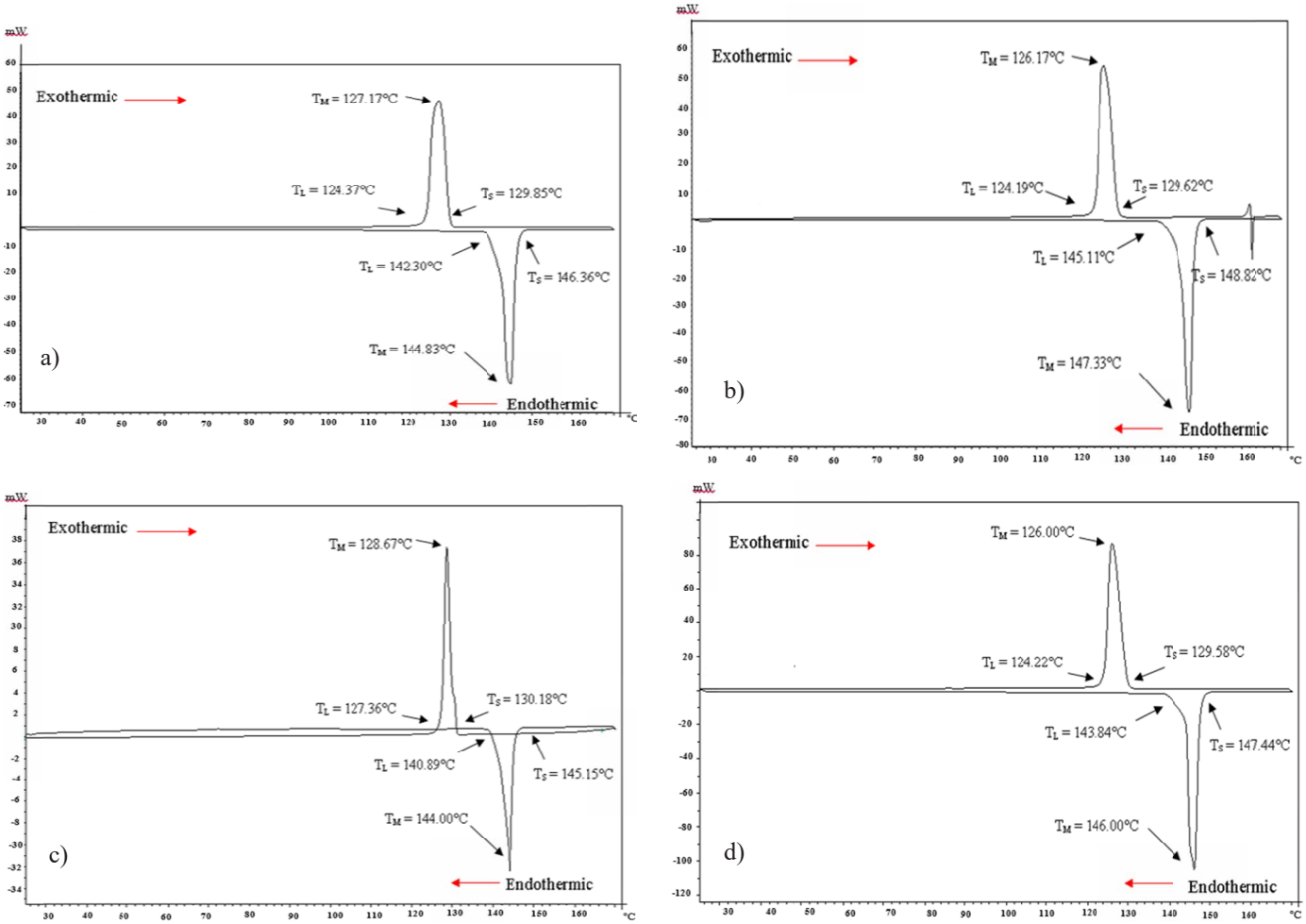

Fig. 4. DSC peak of a) SB, b) SB + 1% ZrO_2, c) SB + 2% ZrO_2 and d) SB + 3% ZrO_2 solder alloy

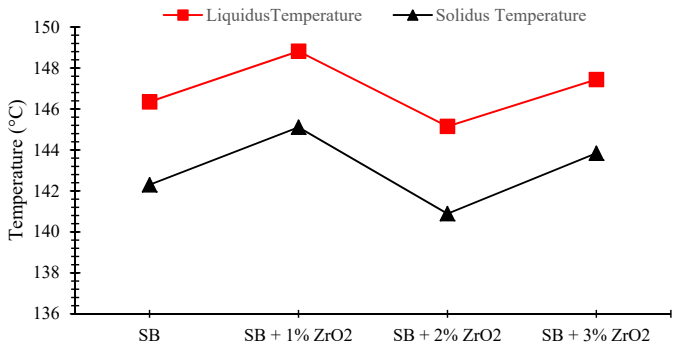

Fig. 5. Solidus and liquidus temperature of SB and SB + ZrO_2 solders at different ZrO_2 nanoparticles concentrations

TABLE 1

Melting properties of SB and SB added nanoparticles solder alloys

Solder	Temperature			Undercooling (°C)	Pasty Range (°C)
	Melting (°C)	Peak (°C)	Liquidus (°C)		
SB	142.30	144.83	146.35	16.51	4.05
SB + 1% ZrO_2	145.11	147.33	148.82	19.2	3.71
SB + 2% ZrO_2	140.89	144.00	145.15	14.97	4.26
SB + 3% ZrO_2	143.84	146.00	147.44	17.86	3.6

has been serving the electronics industry for a long time. Since the melting temperature of the lead solder is 183°C, the melting point of ZrO_2 nanoparticles added into solder alloy in this research was much lower, particularly for 2% addition. In addition, the pasty range of all the nanoparticles solder alloys was less than 5°C, which allowed better microstructure formation of the ZrO_2 added into solder alloys. In a study conducted by [27], the SnZnBiCu solder produced the lowest pasty range of 6.8°C that was proven to provide better microstructures properties. For this study, the highest pasty range was only 4.26°C represented by 2% addition. A narrow pasty temperature is important to allow the solder to exist as liquid in a short time period and allows smaller grain production upon solidification [9]. Moreover, such characteristic avoids any ripping of solder at high temperature [27]. The undercooling is defined as the indicator of the degree of nucleation process. A decrease of 1.5°C was noticed at the addition of 2% ZrO_2, clarifying the ease in the nucleation process to occur. In fact, the increase in the degree of undercooling, unlike the SB solder alloy, was not largely elevated at 1% and 3% ZrO_2 additions, again proving

that ZrO_2 did not change any interatomic spacing between Sn and Bi to drastically change the melting temperature. This is in agreement with the Lindemann's theory. Further effect of this different results on the melting temperature are explained in Section 3.3, namely the agglomeration of particles in 2% ZrO_2 additions. As a result, the mother solder alloy of SnBi became the benchmark for these ZrO_2 nanoparticles added into solders in this study. With the provided results, the variation in melting points, pasty range and undercooling were not large as can be seen in Table 1. As stated, the addition of 2% ZrO_2 nanoparticles produced lower melting point compared to the bare SB solder alloy. The highest melting point was indicated by 1% ZrO_2 added into solder alloy. This is clearly a mixed trend yet this trend is commonly observed by other studies for the addition of different nanoparticles and to be the nature of the nano scale additions [28,29]. The additions of Al_2O_3 nanoparticles in the Sn9Zn solder decreased the melting temperature of the Sn9Zn of ~1°C as reported by [18]. On another note by [30], Al_2O_3 was added to the Sn58Bi solder and showed an increase of ~3°C from the Sn58Bi solder alloy. Similar findings have been reported by [12] and [31]. The explanation for the decrease in 2% ZrO_2 added to SB solder could be related to the presence of ZrO_2, that possesses a higher surface energy that can reach up to 3058 mJ/m^2 [32]. This will increase the surface instability of the molten SB solder alloy which in turn decrease the melting temperature. Contrary to this trend, the increase in the melting temperature is related to the physical characteristics of the nanoparticles being an oxide nanoparticle. These types of nanoparticles have the ability to absorb thermal energy during the melting hence slightly increasing the temperature of the bare SB. Research by [33] stated a similar reason with additions of Fe_2NiO_4 nanoparticles to Sn3Ag0.5Cu. Apart from that, there is a possibility that ZrO_2 nanoparticles affect the melt undercooling before the molten solder solidifies [28].

Therefore, the increases and decreases in temperature during the addition of nanoparticles is a common phenomenon and often discussed in other studies. It should also be noted that the melting properties of a solder is the natural property of the material and influenced by the interatomic space, and any additions of nano scale materials will not affect the melting properties unless it is a larger alloying element addition [34]. Usually, the soldering processes occurs at temperatures ranging 30-40°C higher than the solder alloys melting point. Therefore, higher temperature soldering may damage other components that may need repairing cost. However, importantly, alteration on the current soldering process is not needed for SB solder alloy added with ZrO_2 since the melting properties have no drastic changes.

3.2. Hardness

All three percentages of ZrO_2 added to the SB solder alloy were subjected to indentation to show the ability of the solder to resist deformation. Fig. 6 shows the results of microhardness for each percentage of ZrO_2 addition. From the hardness of SB and SB + ZrO_2 nanoparticles, it clearly indicated that the nanoparticles affected the hardness value. The 1% addition appeared to have a clear increment in the hardness with the highest average value recorded at 32.3 HV. The 2% and 3% ZrO_2 additions recorded averages of 28.5 HV (1% lower than the SB solder) and 27.6 HV (4% lower than the SB solder alloy), respectively. The hardness trend of the solder alloy was as SB + 1% ZrO_2 > SB > SB + 2% ZrO_2 > SB + 3% ZrO_2. The mixed trend indicated that high addition of nanoparticles has reduced the hardness value slightly, in contrast to the bare SB solder alloy. The increase in the hardness value at 1% addition was attributed to the refinement process on the production of smaller grains due to the narrow pasty range recorded for the 1% addition [35,36]. The result of the pasty range from this study obviously indicated that the solidification was rapid and thus the production of smaller grains was imminent. [37] reported similar finding with the presence of Ni nanoparticles in the Sn3.0Ag0.5Cu solder alloy.

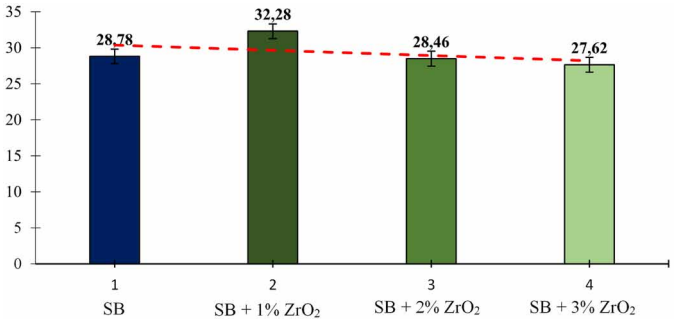

Fig. 6. Vickers microhardness of SB and SB + ZrO_2 solders at different ZrO_2 nanoparticles concentrations

In addition, another possible reason to support the increase in the hardness could be due to the presence of the ZrO_2 nanoparticles itself. The ZrO_2 nanoparticles are discrete and not taking part in any diffusion process, which act as dispersion strengthening mechanism and second phase hardness particles (oxide particles) by the load transfer bearing [38]. This was observed in the scanning electron microscope (SEM) image shown in the latter part of this paper. Such observation was not found on the hardness value for 2% and 3% ZrO_2 additions as there was lower decrease of about 1% to 4% compared to the bare SB solder in the minimum range. The decrease in the hardness can be explained by the presence of high amount of ZrO_2 nanoparticles. By observing the melting behaviour of the 2% ZrO_2 addition, the pasty range was higher that it would not influence the production of smaller grains to enhance the hardness property [39]. The pasty range of the 2% ZrO_2 addition was also close to the pasty range of the bare SB solder alloy, which was also included with the close average hardness result obtained for the 2% ZrO_2 added to SB and the bare SB solder alloy. A study by [19] discovered that the addition of 0.6% ZrO_2 and graphene nanoparticles in the Sn3.0Ag0.5Cu expanded the pasty range and increased the β-Sn size. This will allow easy penetration of the load when indentation is introduced [40] as illustrated in Fig. 7.

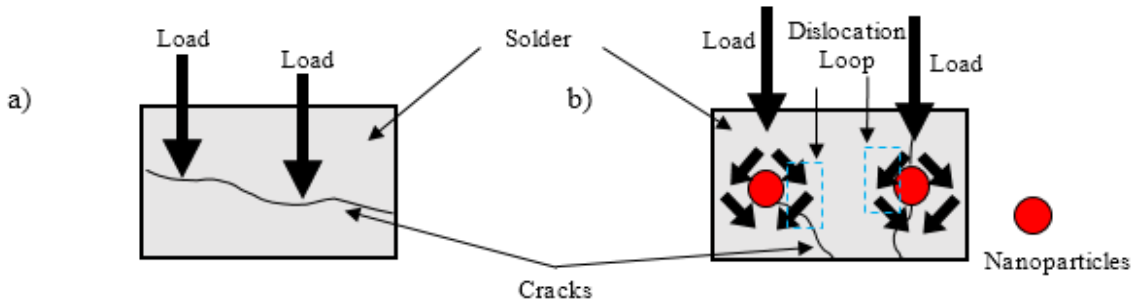

Fig. 7. Load penetration a) without nanoparticles, b) with ZrO_2 nanoparticles

3.3. Microstructural properties

The microstructures of the bare SB and SB + 1, 2 and 3% ZrO_2 nanoparticles are shown in Figs. 8. There was a mixed trend in all three percentages of additions which agrees to the DSC curves noted earlier. The microstructural observation gave vital information that can be related to the hardness of the solder alloy. Certainly, the microstructure of the bare SB solder alloy was altered by the ZrO_2 nanoparticles. Before investigating the alteration, the microstructure of the bare SB solder alloy was analysed as shown in Figs. 8. The presence of lamellar type Sn and Bi structure was identified with the energy dispersive X-Ray (EDX) analysis. This also confirmed the phases as observed in the common SnBi phase diagram in several studies.

Further additions of ZrO_2 nanoparticles altered the primary microstructure of the bare SB solder alloy. In all three percentages of addition, ZrO_2 proved to be mixed with the solder alloy as shown in the average weight elemental detection by the EDX as shown in Table 2. However, it was visible that the ZrO_2 nanoparticles did not entrap in the solder matrix but appeared as if being pushed to the top by the Sn and Bi matrix of lamellar structure. The ZrO_2 nanoparticles have no solubility and do not react with β-Sn and Bi. A study by [41] concluded the reinforcement of the Mo nanoparticles in Sn3.8Ag0.7Cu solder alloy with similar incidence. The addition of 1% ZrO_2 nanoparticles in the SB solder alloy altered the microstructure as the lamellar structure was finer and uniform. Meanwhile, for the 2% ZrO_2 nanoparticle addition, the lamellar structure seemed to be suppressed by approaching alternating gaps as seen in the region highlighted in red in Fig. 8(c). At the same time, the ZrO_2 nanoparticles appeared to accumulate around this region and that led to the near lamellar structure production. However, some presence of agglomeration was noted in the 2% ZrO_2 additions away from the near lamellar structure, showing not all the particles take part in the refinement the microstructure. This was in agreement to the higher pasty range and the lower undercooling reported earlier. Literally, as reported in a few studies [38,42,43], nanoparticles accumulate at high-energy site in the molten solder (e.g. grain boundary). The ZrO_2 nanoparticles present in the SB solder alloys serve as heterogeneous nucleation sites for β-Sn phase and eutectic phase (Sn and Bi phase) and opt to decrease the thermodynamic energy needed for nucleation process [18]. This will increase the nucleation rate of the grains in the solder and reduce the size of grains. In this study, it was indicated by the suppression of the lamellar structure of the ZrO_2 containing solder especially for the 1% and 3% additions, in agreement with [13]. This correlates with the higher degree of undercooling for both percentage of additions. Similar finding has been reported by [44] on the addition of CeO_2 nanoparticles. This occurrence is termed as surface absorption theory which defines that the plane with the maximum surface tension grows the fastest (acting as the nucleation site) with an increased adsorption element (ZrO_2 nanoparticles) as well as nanoparticles; the surface energy and the growth velocity of the plane (β-Sn matrix) will be reduced together [11]. The ZrO_2 nanoparticles did not react with the Sn and Bi in this study and helped in refining of the grain sizes, as observed in previous study [16] cited in Section 1. In fact, various researches that have also studied nanoparticles reinforcement provided similar explanations [14,45]. Nevertheless, in the 2% ZrO_2 additions, there was an opposing trend of decrease in the melt undercooling that would increase the surface energy. This could be due to the micro sized agglomerations noted in the 2%

TABLE 2

Average elemental detection from EDX of a) SB, b) SB + 1% ZrO_2, c) SB + 2% ZrO_2 and d) SB + 3% ZrO_2

a)

Elements	Average Wt %	Average At %
Bi	86.92	76.93
Sn	12.81	19.96

b)

Elements	Average Wt %	Average At %
Zr	08.39	06.77
Bi	14.24	05.02
Sn	67.62	41.99

c)

Elements	Average Wt %	Average At %
Zr	31.55	22.67
Bi	19.12	06.00
Sn	37.73	20.84

d)

Elements	Average Wt %	Average At %
Zr	41.20	26.11
Bi	30.16	08.34
Sn	13.40	06.53

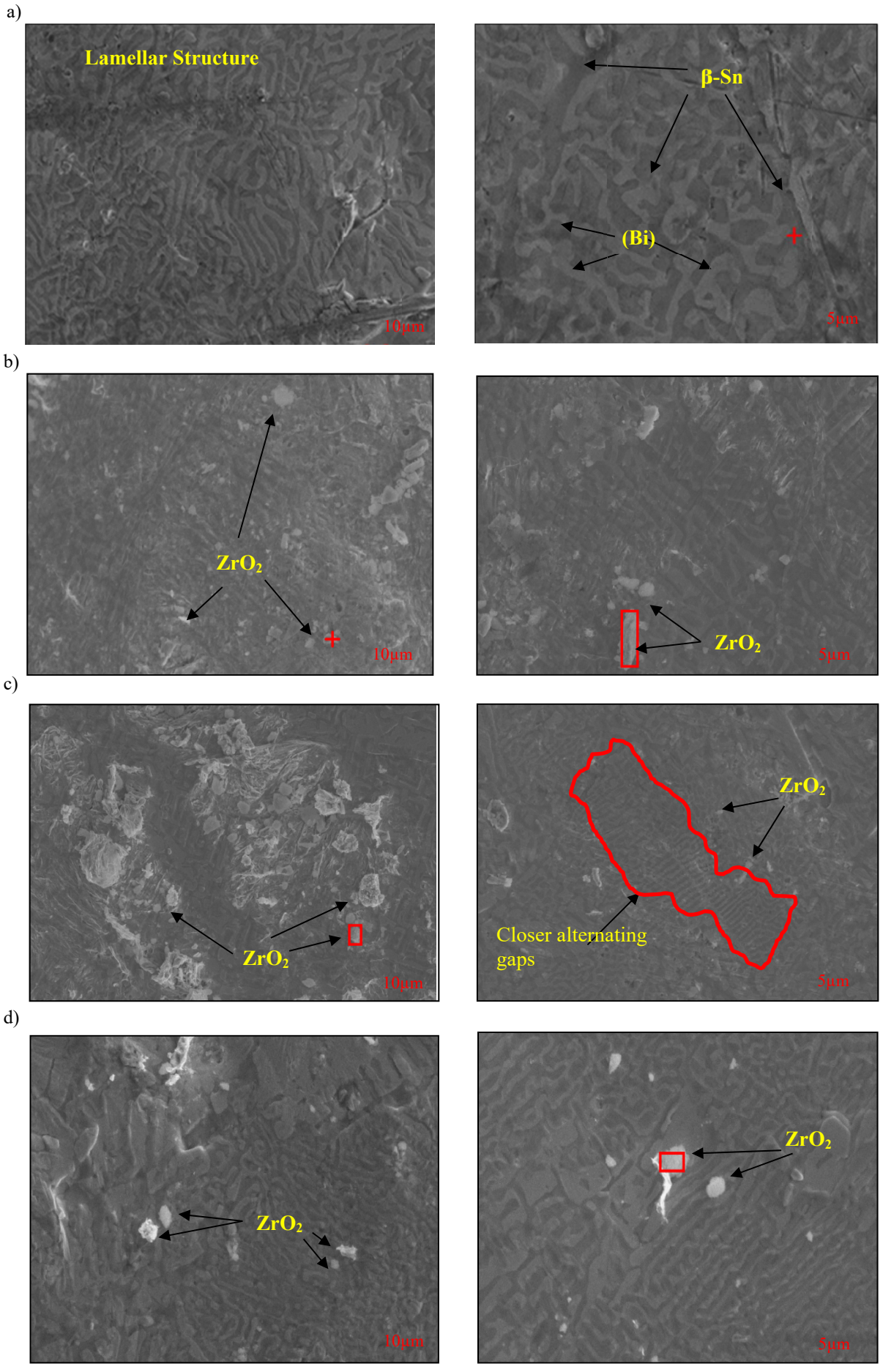

Fig. 8. SEM microstructures image of a) SB, b) SB + 1% ZrO_2, c) SB + 2% ZrO_2 and d) SB + 3% ZrO_2 solder alloy

ZrO_2 additions as in Fig. 8(c). Hence, proper segregation and mixing at different amount of nanoparticles additions contributes to the undercooling that impacts the surface energy.

The representation of the influence of ZrO_2 was modelled as depicted in Fig. 9. This characteristic also contributed to the higher hardness value obtained by the 1% nanoparticles addition compared to the bare SB, 2% and 3% additions. Although ZrO_2 acts as reinforcing particles to the SB solder, the refining of microstructure will be an additional feature for increased hardness. There was greater presence of ZrO_2 nanoparticles in the 2% and 3% addition which was agglomerated as depicted in Fig. 9(c), which will be less effective due to the refinement of microstructure found at lower percentage of addition. Although the presence of ZrO_2 nanoparticles acted as additional load bearing particles, without further microstructure refining function (as 1%), the hardness could not be increased.

3.4. Shear strength

The study of shear strength is essential to distinguish and evaluate the joint reliability of a solder joint. A few studies have focused on this area [46,47]. Table 3 represent the shear load of the SB and SB added with ZrO_2 nanoparticles solder alloy joint. The addition of ZrO_2 nanoparticles showed a distinctive reading on the load at the maximum shear stress. The highest load was recorded for the 3% ZrO_2 added in SB followed by the bare SB, 1% ZrO_2 and 2% ZrO_2 added in the SB solder. It seemed that the addition of 3% ZrO_2 influenced high load and shear stress but the addition of 2% and 1% ZrO_2 produced low load and shear stress values. Figs. 10 show the SEM/EDX of the solder joint interface which clarifies the presence of the ZrO_2 nanoparticles at the IMC layer for all weight percentage additions. The IMC layer thicknesses of the joints were measured as shown in Figs. 11 and the result provides resemblance to the shear stress. The thinnest IMC layer (0.2691 μm) for the 3% ZrO_2 additions possessed the highest shear stress, while the thickest IMC layer (0.9112 μm) for the 1% ZrO_2 additions contributes to the lowest shear stress. If compared to the hardness results earlier, the trend was opposite to the maximum shear strength at joint. This trend actually defined that the addition of 1% and 2% ZrO_2 nanoparticles was mostly concentrated in the solder side (contributing to hardness), whereas the nanoparticles in the 3% ZrO_2 addition mostly concentrated in the solder joint side (contributing to higher shear stress). These could be the possible explanation for the high load increase. The shear stress is directly

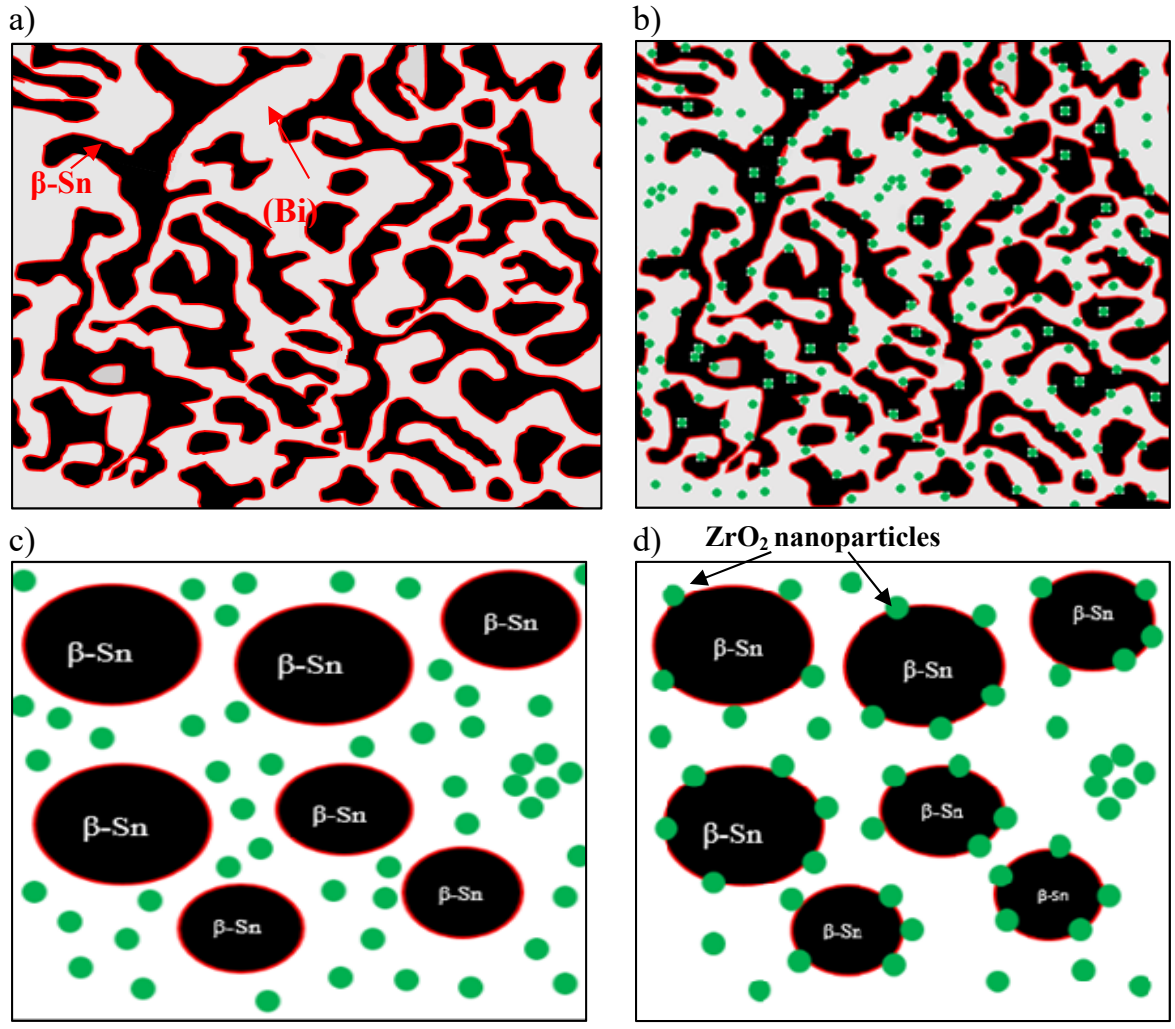

Fig. 9. a) β-Sn and (Bi) matrix, b), c) presence of 1%, 2% and 3% ZrO_2, and d) absorption of 1%, 2% and 3% ZrO_2

a)

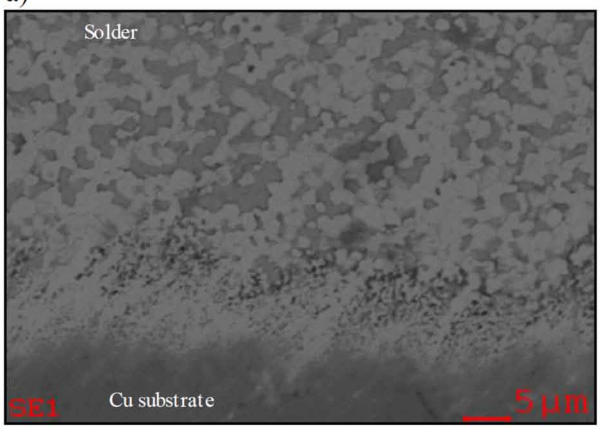

Element	Average Wt. %	Average At. %
Bi	53.56	37.61
Sn	26.89	29.23
Cu	19.56	33.73

b)

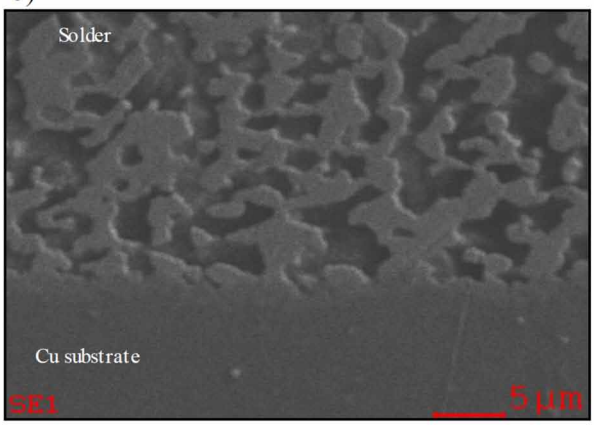

Element	Average Wt. %	Average At. %
Zr	3.75	6.93
Bi	61.90	47.49
Sn	24.24	24.69
Cu	2.93	7.35

c)

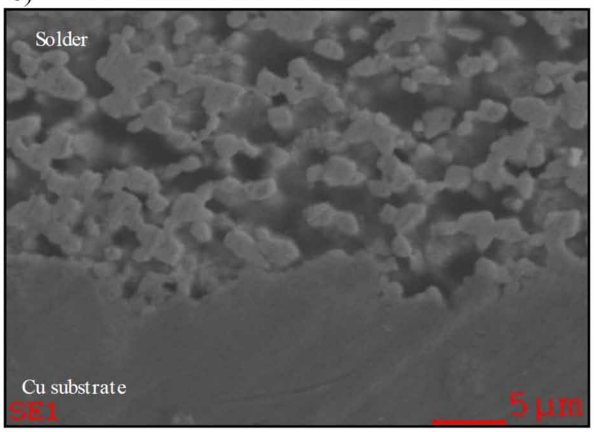

Element	Average Wt. %	Average At. %
Zr	1.83	2.60
Bi	47.70	30.61
Sn	39.55	27.09
Cu	10.97	39.69

d)

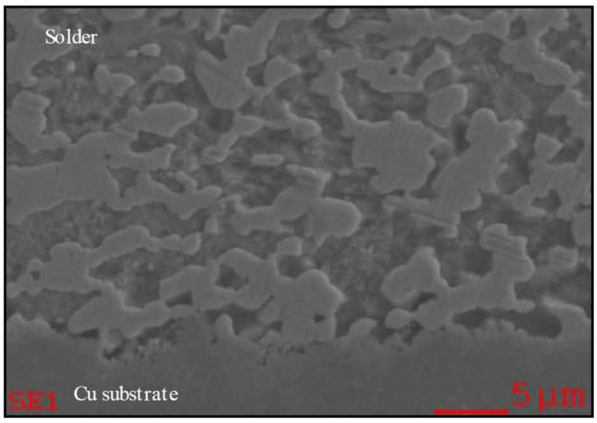

Element	Average Wt. %	Average At. %
Zr	0.67	0.97
Bi	49.72	35.25
Sn	25.19	29.05
Cu	24.42	34.73

Fig. 10. SEM microstructures image with EDX at solder joint of a) SB, b) SB + 1% ZrO_2, c) SB + 2% ZrO_2 and d) SB + 3% ZrO_2 solder alloy

related to the joint interface where the IMC layers are produced between the solder and the substrate [24]. The accumulation of ZrO_2 nanoparticles between the solder and substrate is crucial as the shearing will be induced at that region. Thus, ZrO_2 will inhibit an easier shearing of the joint by enduring a barrier that improves the joint reliability. The results from this study has close agreement with previous studies of [7] and [16], with the latter study recorded shear strengths approximated 43 MPa for 1.0 wt.% and 36 MPa for 0.5 wt.% of ZrO_2 additions in the Sn3.0Ag0.5Cu signifying that the higher percentages of additions contribute to higher shear strength. A study carried out by [48] also reported the enhancement in the shear strength with carbon nanotube (CNT) addition to the SnSb solder system. In addition, another reason may be due to the high-density dislocation provided by the ZrO_2 nanoparticles. The ZrO_2 particles at the solder joint were difficult to pass through which resulted in high dense dislocations that concurrently increased the strength. Comparably, the ZrO_2 additions into the Sn3.0Ag0.5Cu increased the shear stress because of the strengthened solder joint with the ZrO_2 nanoparticles serving as second phase dispersion strengthening mechanism [49]. Similar trend was found by [24] on the addition of Mo nanoparticles in the SnBi solder system. The increase in strength mechanism is known as Orowan strengthening [50].

TABLE 3

Maximum load of SB and SB added nanoparticles solder joint

Solder	Trials	Shear Strength (kN)	Average (kN)
SB/Cu	1	0.7383	**0.5145**
	2	0.2484	
	3	0.4605	
	4	0.5206	
	5	0.6047	
SB + 1% ZrO_2/Cu	1	0.4423	**0.4380**
	2	0.3298	
	3	0.5417	
	4	0.3161	
	5	0.5603	
SB + 2% ZrO_2/Cu	1	0.2936	**0.4863**
	2	0.3823	
	3	0.5598	
	4	0.4338	
	5	0.7620	
SB+ 3% ZrO_2/Cu	1	0.8432	**0.8712**
	2	0.8979	
	3	0.7142	
	4	1.1192	
	5	0.7817	

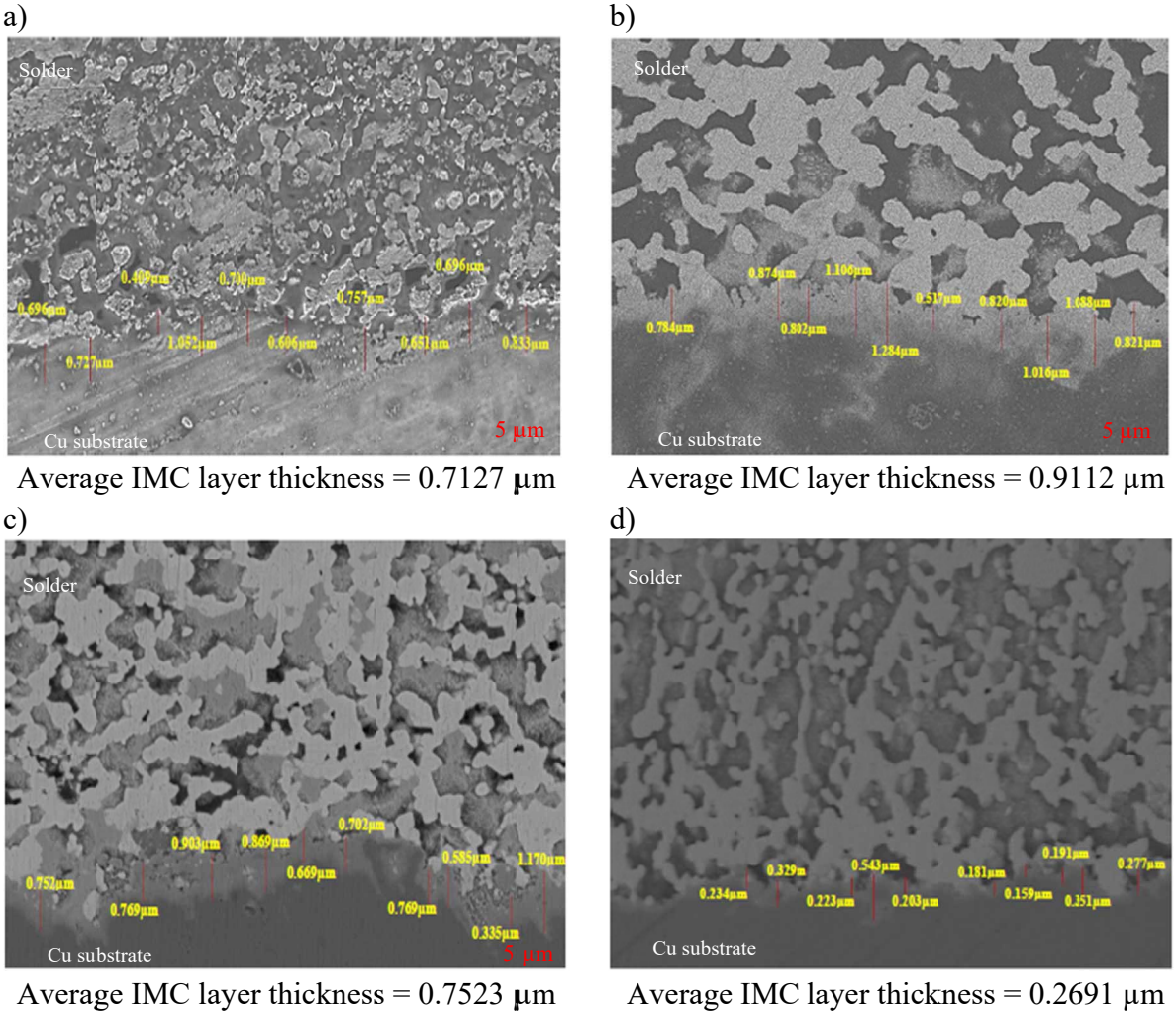

Fig. 11. SEM morphology and IMC layer thickness of a) SB, b) SB + 1% ZrO_2, c) SB + 2% ZrO_2 and d) SB + 3% ZrO_2 solder joints

4. Conclusion

This study reveals the effect of different percentage of ZrO_2 nanoparticles added in the SB solder alloy. Based on the results obtained, these conclusions can be withdrawn:

1. The ZrO_2 nanoparticles did not involve in any diffusion process (at 600°C) which clarified its impact as discrete particles. These results correlated with the microstructure and mechanical properties of the solder alloy.
2. Melting temperature of all three percentages of ZrO_2 addition in SB showed mixed pattern at a minimum range (≈2°C), unlike the reference temperature of SB (142.30°C). This criterion is important to maintain a lower reflow soldering temperature.
3. Microstructures of the SB were altered with the addition of ZrO_2 nanoparticles and there was a production of nearer lamellar gaps as the ZrO_2 acted as a heterogeneous nucleation site.
4. Mechanical properties of hardness and shear strength of SB + 1%, 2% and 3% ZrO_2 solder alloys also showed mixed pattern. The presence of nanoparticles in the solder side contributed to the hardness property and the 1% ZrO_2 addition indicated higher value due to additional strengthening mechanism. In contrary, the % ZrO_2 addition obtained higher load at the joint as the shear properties were affected by the solder joint strength. This showed that at higher ZrO_2 particles addition, the nanoparticles tended to accumulate at the solder joint, increased the shear strength, acted as load bearing particles and obstacles for motion of dislocations.

Proper mixing of ZrO_2 nanoparticles in the SB solder alloy seemed to improve the microstructural and mechanical properties as found in this study. Insignificant alteration was performed on the melting temperature. This study also provides a relevant summary on the behaviour of nanoparticles in the solder alloy and the mechanism to enhance the strength. This information can be an additional guideline for future studies acts as good literature to other studies in similar field.

REFERENCES

[1] L. Zhang, K.N. Tu, Mater. Sci. Eng. R. **82**, 1-32, (2014).

[2] F. Gnecco, E. Ricci, S. Amore, G. Borzone, R. Novakovic, Int. J. Adhes. Adhes. **27** (5), 409-416 (2007).

[3] A.K. Gain, L Zhang, J. Mater. Sci.: Mater. Electron. **27** (11), 11273-11283 (2016).

[4] Y.W. Wang, Y.W. Lin, C.T. Tu, C.R. Kao, J. Alloys Compd. **478**, 121-127 (2009).

[5] A.K. Gain, L. Zhang, J. Mater. Sci.: Mater. Electron. **27** (7), 7524-7533 (2016).

[6] L.C. Tsao, S.Y. Chang, Mater. Des. **31**, 990-993 (2010).

[7] J. Shen, Y.C. Chan, Microelectron Reliab. **49**, 223-234 (2009).

[8] S. Cheng, C.-M. Huang, M. Pecht, Microelectron Reliab. **75**, 77-95 (2017).

[9] H.R. Kotadia, P.D. Howes, S.H. Mannan, Microelectron Reliab. **54**, 1253-1273 (2014).

[10] M.D. Abtew, G. Selvaduray, Mater. Sci. Eng. **27**, 95-141 (2000).

[11] M.N. Ervina Efzan, A. Singh, Solder Surf. MT. Tech. **26** (3), 147-161 (2014).

[12] M.A.A. Mohd Salleh, S.D. Mcdonald, K. Nogita, J. Mater. Process. **24**, 235-245 (2017).

[13] S. Chellvarajoo, M.Z. Abdullah, Microelectron Reliab. **84**, 230-237 (2018).

[14] J. Wu, S. Xue, J. Wang, M. Wu, J. Wang, J. Mater. Sci. Mater. **29**, 7372-7387 (2018).

[15] P. Yao, X. Li, X. Han, L. Xu, Solder Surf. MT. Tech. **31** (1), 6-19 (2019).

[16] A. Yakymovych, Yu. Plevachuk, P.S. Vec Sr, P.S. Vec, D. Janickovic, P.S. Ebo, N. Beronska, A. Roshanghias, H. Ipser, J. Electron. Mater. **45** (12), 6143-6149 (2016).

[17] A. Singh, R. Durairaj, Effect on the wettability, hardness and shear strength properties of 3%-nano Titanium Oxide (TiO_2) added Sn-3.8Ag-0.7Cu (SAC)/Copper (Cu) solder joint, MATEC Web of Conferences. **237** (02013), (2018).

[18] W.-Q. Xing, X. Yu, H. Li, L. Ma, W. Zuo, P. Dong, J. Alloys Compd. **695**, 574-582 (2017).

[19] Y. Tang, G. Li, Y. Pan, Mater. Des. **55**, 574-582 (2014).

[20] Y. Tang, S.M. Luo, W.F. Huang, Y.C. Pan, G.Y. Li, J. Alloys Compd. **719**, 365-375 (2017).

[21] F. Khodabakhshi, R. Sayyadi, N.S. Javid, Mater. Sci. Eng. **702**, 371-385 (2017).

[22] Y. Ma, X. Li, L. Yang, W. Zhou, M. Wang, W. Zhu, P. Wu, Mater. Sci. Eng, **696**, 437-444 (2017).

[23] Y. Li, Y.C. Chan, J. Alloys Compd. **645**, 566-576, (2015).

[24] L. Yang, L. Zhu, Y. Zhang, S. Zhou, Z. Wang, S. Shen, X. Shi, Mater. Charact. **148**, 280-291 (2019).

[25] S. Zhou, O. Mokhtari, M.G. Rafique, C.V. Shunmugasamy, B. Mansoor, H. Nishikawa, J. Alloys Compd. **765**, 1243-1252 (2018).

[26] Y.-L. Tsai, W.-S. Hwang, Mater. Sci. Eng. A. **413-414**, 312-316 (2005).

[27] F. Xing, X.-M. Qiou, Y.-d. Li, Trans. Nonferrous Met. Soc. China. **25**, 879-884 (2015).

[28] D.-H. Jung, A. Sharma, J.-P. Jung, J. Alloys Compd. **743**, 300-313 (2018).

[29] S. Chellvarajoo, M.Z. Abdullah, C.Y. Khor, Mater. Des. **82**, 206-215 (2015).

[30] S. Amares, M.N. Ervina Efzan, R. Durairaj, A. Niakan. Influence of Nano-3%Al_2O_3 on the Properties of Low Temperature Sn-58Bi (SB) Lead-free Solder Alloy, IOP Conf. Ser.: Mater. Sci. Eng. **205** (012002), (2017).

[31] Z.L. Li, G.Y. Li, B. Li, L.X. Cheng, J.H. Huang, Y. Tang, J. Alloys Compd. **685**, 983-991 (2013).

[32] Z. Moser, W. Gasior, J. Pstrus, J. Electron. Mater. **30**, 1104-1111 (2011).

[33] S. Chellvarajoo, M.Z. Abdullah, Z.Samsudin, Mater. Des. **67**, 197-208 (2015).

[34] K. Kanlayasiri, N. Meesathien, Adv. Mat. Sci. Eng. **33**, 1-10 (2018).

[35] Z. Fathiana, A. Malekib, B. Niroumand. Ceram. Int. **43**, 5302-5310 (2017).
[36] M. Ding, W. Xing, X. Yu, L. Ma, W. Zuo, Z. Ji, J. Alloys Compd. **739**, 481-488 (2018).
[37] A.K. Gain, L. Zhang, Acta Mater. **5**, 100234 (2019).
[38] S. Shang, Y. Wang, Y. Wang, H. Ma, A. Kunwar, Microelectron. Eng. **208**, 47-53 (2019).
[39] G. Chen, H. Peng, V.V. Silberschmidtet, Y.C. Chan, C. Liu, F. Wu, J. Alloys Compd. **685**, 680-689 (2016).
[40] Y. Lu, L. Ma, S.-y. Li, W. Zuo, Z.-q. Ji, M. Ding, J. Alloys Compd. **765**, 128-139 (2018).
[41] A. Haseeb, M.M. Arafat, M. Rafie Johan, Mater. Charact. **64**, 27-35 (2012).
[42] A.E. Hammad, Mater. Des. **50**, 108-116 (2013).
[43] B.X. Voung, N.S.H. Vu, T.D. Manh, M. Vaka, D.X. Du, N.D. Nam, Mater. Lett. **208**, 309-313 (2018)
[44] Z.H. Li, Y. Tang, Q.W. Guo, G.Y. Li, J. Alloys Compd. **789**, 150-162 (2019).
[45] X. Hu, Y. Yang, S. Xu, Z. Chen, Mater. Sci. Eng. **600**, 67-75 (2014).
[46] Y. Zuo, J. Shen, J. Xie, Xiang Lu, J. Mater. **257**, 250-256 (2018).
[47] L. Yang, W. Zhou, Y. Ma, X. Li, Y. Li, W. Cui, P. Wu, Mater. Sci. Eng. **667**, 368-375 (2016).
[48] O. Mokhtari, H. Nishikawa. Mater. Sci. Eng. **651**, 831-839 (2016).
[49] A.K. Gain, Y.C. Chan, K.C. Yung, Microelectron Reliab. **51**, 2306-2313 (2011).
[50] T.T. Dele-Afolabi, M.A. Azmah Hanim, M. Norkhairunnisa, H.M. Yusoff, M.T. Suraya, J. Alloys Compd. **649**, 368-374 (2015).